Colloid Polym Sci (2009) 287:501–504
DOI 10.1007/s00396-009-2013-4

SHORT COMMUNICATION

Atom transfer radical polymerized PMMA/magnetite nanocomposites and their magnetorheology

Bong Jun Park · Min Ki Hong · Hyoung Jin Choi

Received: 2 January 2009 / Accepted: 1 February 2009 / Published online: 25 February 2009

Abstract We synthesized core/shell-typed magnetic nanoparticle composites using poly(methyl methacrylate) (PMMA) as a shell and magnetite nanoparticle (MN) as a core, in which the PMMA shell was prepared via atomic transfer radical polymerization (ATRP) method. Chemical structure and morphology of the synthesized MN–PMMA nanocomposite were investigated using FT-IR and TEM, respectively. Magnetorheological (MR) fluid was prepared by dispersing synthesized MN–PMMA in non-magnetic medium. Both shear stress and shear viscosity of the MR fluids as a function of shear rate were measured using a rotational rheometer with a magnetic field generator, exhibiting that a yield stress increased with an external magnetic field strength.

Keywords Nanocomposite · Magnetite · Magnetorheological fluid · ATRP · Core–shell

Introduction

Magnetorheological (MR) fluid, one of the smart and intelligent materials with controllable properties by an external magnetic field, consists of magnetic particles dispersed in a non-magnetic fluid medium [1, 2]. In the absence of an applied external magnetic field, MR fluids show a Newtonian fluid behavior such that shear stress increases linearly with shear rate. However, when an external magnetic field is being applied, the fluid transforms from a liquid-like to a solid-like state very rapidly because the magnetic particles in fluid form fibrillar structures along the magnetic field direction by their dipole interaction induced by the applied magnetic field [3–7]. Furthermore, as soon as an external magnetic field is removed, the fluid quickly and reversibly returns to a freely flowing original liquid state. This change of fluid state with external magnetic field makes the rheological properties of the MR fluids unique [8]. Particles for MR fluids should be magnetized under an external magnetic field, meaning that ferromagnetic, ferrimagnetic, and paramagnetic materials can be, in general, adapted as a dispersed phase of MR fluids. In addition, soft magnetic materials which are easy to be magnetized and demagnetized are superior to hard magnetic materials, considering the reversible control of rheological properties of MR fluids according to external fields.

Therefore, MR fluids become important materials for various engineering applications [9, 10]. In this study, as a new MR material, we synthesized core–shell-typed magnetite MN–PMMA nanoparticle nanocomposites by an atomic transfer radical polymerization (ATRP) method to resolve sedimentation and abrasion problems induced by the high density and rigid surface of the MN [11]. As a result, it was confirmed that the density of synthesized magnetite MN–PMMA nanoparticle decreased compared with that of MNs and aggregation among magnetic particles were reduced. Furthermore, rheological properties of the MR fluid were investigated.

Experimental

The MN–PMMA magnetic nanocomposites were synthesized following the three-step process. At first, the MNs were produced by a co-precipitation method of an aqueous Fe^{3+}/Fe^{2+} solution with a base. Ferric chloride

B. J. Park · M. K. Hong · H. J. Choi (✉)
Department of Polymer Science and Engineering, Inha University, Incheon 402-751, South Korea
e-mail: hjchoi@inha.ac.kr

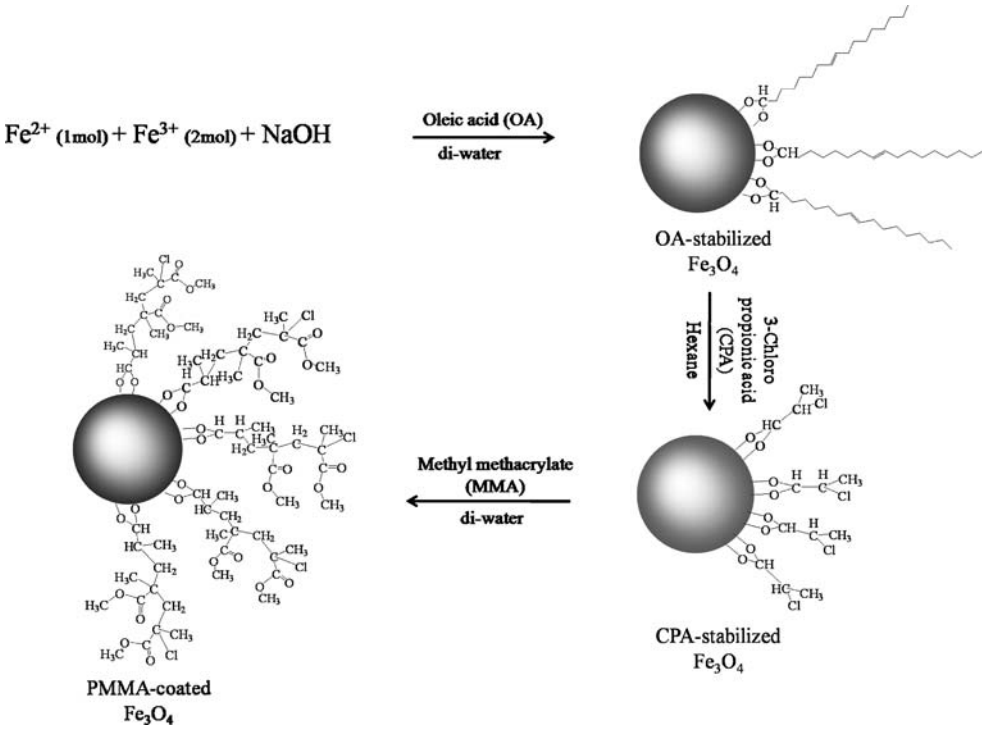

Fig. 1 Synthesis route of PMMA-coated Fe_3O_4

hexahydrate ($FeCl_3 \cdot 6H_2O$) and ferrous sulfate heptahydrate ($FeSO_4 \cdot H_2O$) were dissolved in distilled water and heated to 60ºC. Then, ammonium hydroxide and oleic acid (OA) were added rapidly under stirring for 30 min, and the temperature of the reactor was decreased to room temperature. After 6 h, the precipitates were washed several times with distilled water and methanol. After being dried in the vacuum oven at 80ºC, the dark brown powder was obtained. As the second step, initiators were immobilized on the surface of MNPs. Prepared MNs which were stabilized by the OA were put in hexane. In order to disperse the MNs in hexane, the mixture was sonicated for 1 h. Another initiator, 3-chloropropionic acid (CPA), was also added in the mixture, and the mixture was kept stirred and sonicated. After 1 day, the precipitates were separated from the mixture by centrifugation. Excess CPA was removed through washing with hexane several times. After being dried in the vacuum oven at 80ºC, MNs with CPA immobilized on their surface were obtained. In the last step, the MN–PMMA nanocomposites were synthesized via a surface-initiated atomic transfer radical polymerization of MMA [12, 13]. Prepared MNs–CPA was dispersed in toluene and the mixture was sonicated for 1 h. Then, MMA monomer, 2,2-dipyridyl (bpy), and copper(I) bromide (CuBr) were then added altogether in the mixture, and the mixture was sealed in a glass reactor. The mixture was purged with nitrogen for 1 h and vigorously stirred. Surface-initiated ATRP was carried out at 80ºC with stirring for 1 day. The precipitates were washed with toluene by centrifugation and a magnet. Finally, the precipitates were dried in vacuum oven at 80ºC and red brown final product particles of the MN–PMMA were obtained. The synthesis route of the MN–PMMA is shown in Fig. 1.

The chemical structures of MN, MN–CPA, and MN–PMMA were investigated by Fourier transform infrared spectrometer (FT-IR, VERTEX, Bruker Optics, USA), in which the spectrum was taken between 400 and 4,000 cm^{-1} with 16 scan at a resolution of 8 cm^{-1}. Morphologies of the MN, MN–CPA, and MN−PMMA were observed by using

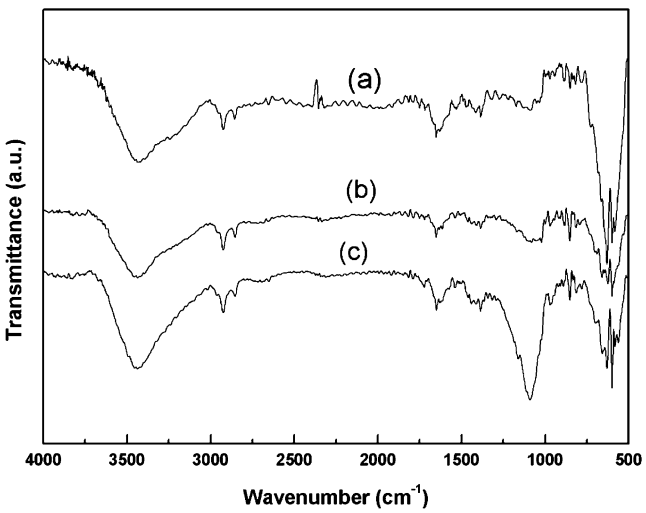

Fig. 2 FT-IR spectra of (*a*) MN–OA, (*b*) MN–CPA, and (*c*) MN–PMMA

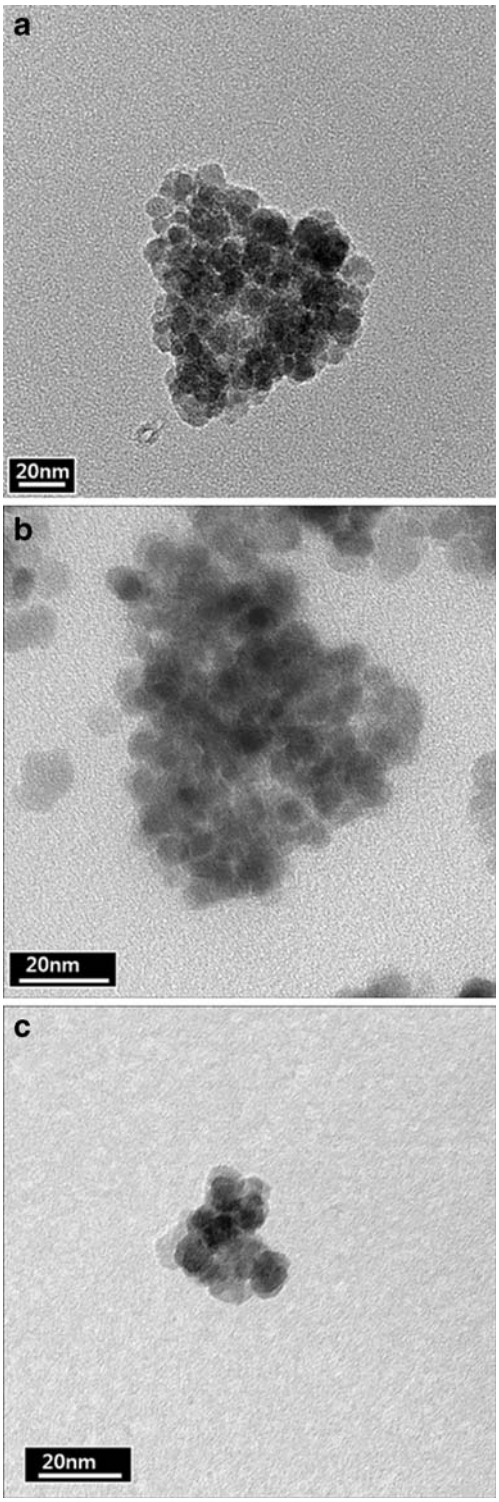

Fig. 3 TEM images of **a** MN–OA, **b** MN–CPA, and **c** MN–PMMA

transmission electron microscopy (TEM, CM200, Philips, USA). The magnetic particles were then dispersed in medium lubricant oil (Yubase8, SK, Korea). The rheological properties of the MR fluid were characterized by using a rotational rheometer (MCR300, Physica, Germany) with the MR device (MRD 180). A parallel-plate measuring system with a diameter of 20 mm was used at a gap distance of 1 mm.

Results and discussion

The FT-IR spectra of (a) MN–OA, (b) MN–CPA, and (c) MN–PMMA are shown in Fig. 2. The strong peak between 590 and 630 cm^{-1} was attributed to the Fe–O bond of the MN. The presence of this peak means that the Fe_3O_4 particles were synthesized successfully by co-precipitating an aqueous Fe^{3+}/Fe^{2+} solution. Two peaks around 2,930 and 2,850 cm^{-1} were attributed to the asymmetric CH_2 stretch and the symmetric CH_2 stretch, respectively. Another peak around 1,660 cm^{-1} indicates the characteristics of the C═O double bond stretching. These results imply that the surface of MNPs was coated by the oleic acid successfully. On the other hand, the strong absorption band

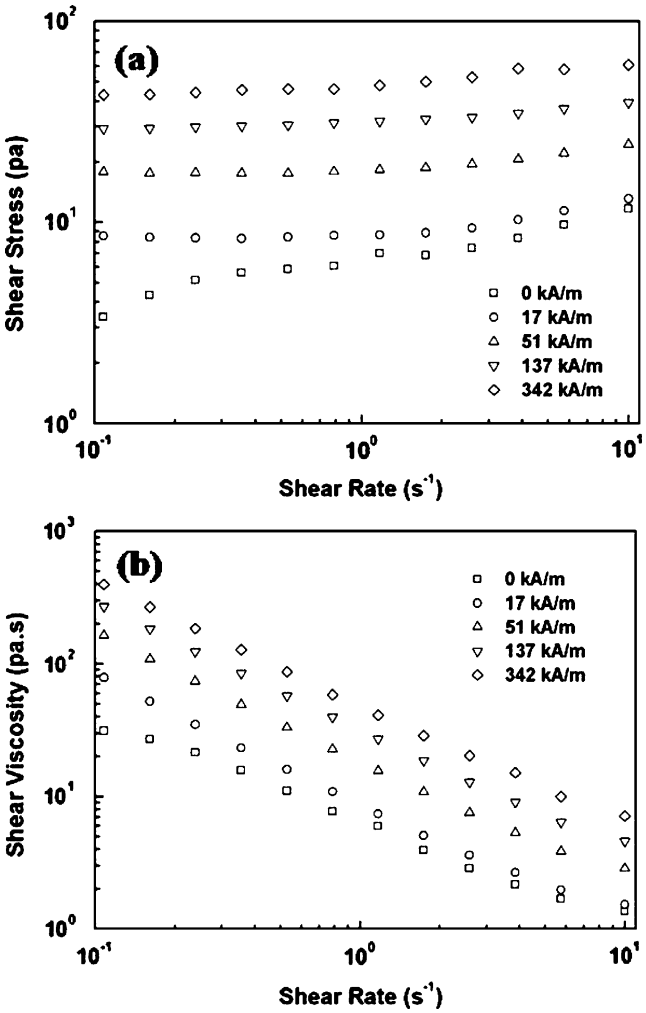

Fig. 4 **a** Shear stress and **b** shear viscosity as a function of shear rate for MR fluid at different magnetic strengths

around 1,090 cm^{-1} was observed in curve (c). This strong absorption band was attributed to the C–O–C ether stretch of PMMA, implying that the PMMA was coated on the surface of MN.

TEM images of (a) MN–OA, (b) MN–CPA, and (c) MN–PMMA given in Fig. 3 show that the MN–OA, MN–CPA, and MN–PMMA have a practically spherical shape with uniform particle size of 8–15 nm. Because the particles are aggregated and the contrast difference between PMMA and background in Fig. 3 is not very distinctive, it is not easy to find PMMA coating layers of the MN–PMMA directly. On the other hand, aggregation of the MN–PMMA, MN–OA, and MN–CPA was observed. Compared with aggregated MN possessing very high surface energy, the MN–PMMA of which their surface energy was reduced by coated surface of MN with PMMA were less aggregated than both MN–OA and MN–CPA. Though the PMMA coating layer could not be observed, it was indirectly confirmed that the MN was coated by the PMMA.

The MR fluid was prepared by dispersing synthesized MN–PMMA in non-magnetic medium of Yubase8 by 10 vol.%. Its rheological properties were then measured by using a rotational rheometer. Shear stress as a function of shear rate for the MR fluid under different external magnetic field strengths was shown in Fig. 4a. At zero magnetic field strength, the MR fluid acted like general suspension which shows increased shear stress with increasing shear rate. However, when the external magnetic field was applied to the MR fluid, it behaved like Bingham fluid [14, 15] with a yield stress because the MN–PMMA in the medium formed particle chains or particle cluster by polarization force between particles under magnetic field strength. The yield stress of the MR fluid increased from 8 to 40 Pa with increasing external magnetic field from 17 to 343 kA/m. The polarization force induced by external magnetic field between particles increases with increasing external magnetic field strength. The stronger polarization force between particles makes the stronger particle chains or particle clusters in the MR fluid [16]. In addition, shear stress of the MR fluid remained constant independent of shear rate, because the magnetostatic force induced by external magnetic field between particles is stronger than the hydrodynamic force induced by external flow field. Even if the formed particle chains or particle clusters are destroyed by shear deformation, they are reformed by applied magnetic field. Figure 4b shows the relationship between share viscosity and shear rate. It was confirmed that shear viscosity at low shear rate increases with the external magnetic field strengths. Shear thinning behavior of the viscosity decrease with a shear rate was also observed.

Conclusion

MN–PMMA composites with core and shell type were synthesized by ATRP method. Their chemical structure and morphology were observed by using FT-IR and TEM. When its MR fluids were prepared in non-magnetic medium of Yubase8 with 10 vol.%, it shows typical MR fluid characteristics of Bingham fluid when external magnetic fields were applied. Shear stress of the MR fluid increased with external magnetic field strength, while it was observed to be independent of shear rate in a wide range.

Acknowledgement This work was supported by SK Energy, Korea (2008).

References

1. Lita M, Popa NC, Velescu C, Vekas LN (2004) IEEE Trans Magn 40:469
2. Cho MS, Lim ST, Jang IB, Choi HJ, Jhon MS (2004) IEEE Trans Magn 40:3036
3. Bica I (2007) J Ind Eng Chem 13:299
4. Bombard AJF, Knobel M, Akantara MR (2007) Int J Modern Phys B 21:4858
5. Genc S, Phule PP (2002) Smart Mater Struct 11:140
6. Lim ST, Cho MS, Jang IB, Choi HJ, Jhon MS (2004) IEEE Trans Magn 40:3033
7. Hu B, Fuchs A, Gordaninejad F, Evrensel C (2007) Int J Mod Phys B 21:4819
8. Bica I, Choi HJ (2008) Int J Mod Phys B 22:5041
9. Pu HT, Jiang FJ, Yang Z, Yan B, Liao X (2006) J Appl Polym Sci 102:1653
10. Li WH, Du H, Guo NQ (2004) Mat Sci Eng A 371:9
11. Marutani E, Yamamoto S, Ninjbadgar T, Tsujii Y, Fukuda T, Takano M (2004) Polymer 45:2231
12. Hu B, Fuchs A, Huseyin S, Gordaninejad F, Evernsel C (2006) Polymer 47:7653
13. Zhou Y, Wang SX, Ding BJ, Yang ZM (2008) Chem Eng J 138:578
14. Choi HJ, Kim JW, Joo J, Kim BH (2001) Synth Met 121:1325
15. Hong CH, Choi HJ, Jhon MS (2006) Chem Mater 18:2771
16. Ekwebelam CC, See H (2007) Korea-Australia Rheol J 19:35